THE NON-DARCY CHARACTERISTICS OF FAULT WATER INRUSH IN KARST TUNNEL BASED ON FLOW STATE CONVERSION THEORY

by

Zheng-Zheng CAO[a,b], Yu-Feng XUE[a], Hao WANG[b*], Jia-Rui CHEN[c], and Yu-Lou REN[a]

[a] International Joint Research Laboratory of Henan Province for Underground Space Development and Disaster Prevention, Henan Polytechnic University, Jiaozuo, China
[b] School of Energy Science and Engineering, Henan Polytechnic University, Jiaozuo, China
[c] Faculty of Architecture and Civil Engineering, Huaiyin Institute of Technology, Huai'an, China

Original scientific paper
https://doi.org/10.2298/TSCI2106415C

The fault water inrush is a key factor which leads to tunnel construction in karst regions. Based on the fluid mechanics principles, the paper addresses a numerical coupled model for karst fault tunnel with COMSOL Multiphysics software. Besides, the Darcy law equation, Brinkman equation, and Navier-Stokes equation are inserted to stimulate the steady flow of aquifer, the non-linear seepage of fault and the free flow in tunnel excavating area in software, respectively. Then, the pressure and flow velocity in three flow fields are analyzed under different permeability ratios in numerical model. It is shown that the fault permeability is the key factor affecting water inrush, and that the pressure and flow velocity change visibly in adjacent domains between two flow fields.

Key words: *non-Darcy characteristics, fault water inrush, karst tunnel, flow state conversion theory, coupled model*

Introduction

In the 21st century, China has achieved the remarkable success in the infrastructure projects. The network of roads and railways links every part in China. For the sake of regional development, a large number of tunnel projects have been built [1-3]. Because of the complex geological conditions, inaccurate advance geological prediction and limited construction technology, water inrush disaster occurs in many conditions, which seriously affects the safety of tunnel construction. The fault fracture zone is a type of engineering geology in karst area, influenced by groundwater erosion and excavation disturbance, therefore, the fault fracture zone is easy to become the seepage channel of groundwater [4, 5]. When the tunnel passes through the fault fracture zone, water inrush is easy to occur. Therefore, it is of significance to carry out the analysis of water inrush process of tunnel in karst area, especially in fault fracture zone.

Many experts and scholars have conducted extensive research on the fault water inrush encountered in underground engineer [6]. Li *et al.* [7] investigated the whole process of water inrush from coal floor with fault by finite element numerical simulation, and concluded that the physical properties and occurrence factors of faults have an important influence on the relative safety of coal floor [8]. Liu *et al.* [9] simulated the whole process of mud-stone roof from water

* Corresponding author, e-mail: 695263195@qq.com

isolation to water inrush influenced by mining and water pressure, with the seepage-stress coupling analysis system in rock fracture process. In addition, there are many scholars devoted to the research on fault water inrush. The aforementioned researches mainly analyze the activation process of fault water inrush from its occurrence and physical properties. In terms of hydrodynamics, this is a non-linear seepage process, in which the water in the aquifer flows to the fault, erodes and scours the fine particles, and breaks through the water-proof floor or the palm surface after excavation disturbance [10, 11].

Based on the research background of practical engineering, this paper is to divide the fluid-flow into three stages, namely the laminar flow in aquifer, the non-linear seepage during activation of fracture zone, and the turbulent flow in tunnel. The flow states of three stages are described by the Darcy law, the Brinkman equation, and the Navier-Stokes equation, respectively.

Equations of coupled model

Evolution of water inrush in fault fracture zone

In the original conditions, the fault has no or weak conductivity. When the excavation of the tunnel breaks the stress balance state of the original rock, the fault is gradually activated, cracks in the fracture zone initiate and expand, and the permeable water channel is formed by fluid erosion, and the conductivity is greatly enhanced. Fluids from the aquifer and surrounding rock formations are channeled to the tunnel face. In the process of water inrush, the fluid experiences three physical processes, namely the Darcy laminar flow in aquifer, the Non-Darcy high-speed flow in broken rock mass, and the Navier-Stokes turbulent flow in roadway. Fluid-flow is a unified organism [12, 13]. The pressure and velocity of the three flow fields are in harmony with each other. It can be seen that water inrush from fault is a continuous process. Water inrush disaster is very likely to occur, if the tunnel construction water-proof measures are not in place, or advance geological conditions are difficult to predict.

Governing equation of flow state in three stages

The water inrush process of the fault fracture zone in karst area can be described as Darcy linear flow in aquifer, Brinkman non-linear flow in fractured rock mass and Navier-Stokes turbulent flow in roadway.

The first stage is Darcy linear flow in aquifer. The hydraulic relation between the fluid in the deep rock aquifer and the surrounding rocks is relatively stable, which belongs to low-speed porous media seepage and is mainly driven by fluid pressure, and the fluid inertia force can be ignored. In COMSOL multiphysics, the Darcy law is expressed:

$$\nabla\left(\rho u\right)=Q_m \quad \text{and} \quad u=-\frac{k}{\mu}\nabla p \tag{1}$$

where k is the permeability, p – the fluid pressure, ρ – the fluid density, Q_m – the source and sink term, u – the Darcy velocity, and μ – the dynamic viscosity.

The second stage is Brinkman non-linear flow in fractured rock mass. Brinkman equation is a non-linear seepage equation between Darcy flow and Navier-Stokes flow, which is used to describe the seepage characteristics in fractured fault rock mass. In COMSOL Multiphysics, the Brinkman equation with Forchheimer correction in the porous region is used to describe the flow as:

$$u\left(\frac{\mu}{k}+\beta_{\mathrm{f}}\left|u\right|+\frac{Q_{\mathrm{br}}}{\psi_p{}^2}\right)=\nabla\left\{-pI+\frac{\mu}{\psi_p}\left[\nabla u+\left(\nabla u\right)^T\right]\right\}+F \quad \text{and} \quad \rho\nabla u=Q_{\mathrm{br}} \tag{2}$$

where β_{f} is the non-Darcy factor, ψ_p – the porosity, F – the volumetric force affecting the fluid, and I – the identity matrix. The relation between permeability and non-Darcy factor is given:

$$\beta_{\mathrm{f}}=\frac{\rho\psi_p C_{\mathrm{f}}}{\sqrt{k}} \tag{3}$$

The friction coefficient is:

$$C_{\mathrm{f}}=\frac{1.75}{\sqrt{150\psi_p^3}} \tag{4}$$

where C_{f} is the friction coefficient.

The third stage is Navier-Stokes turbulence in the tunnel face. The fluid reaches the face through the water channel of fault fracture zone. When the amount of water reaches a certain amount and the waterproof and water-proof ability of tunnel face is limited, the fluid can break through the face and enter the roadway to flow freely. This process is in accordance with Navier-Stokes equation as follows [14]:

$$\rho u\nabla u=\nabla\left\{-pI+\mu\left[\nabla u+\left(\nabla u\right)^T\right]\right\}+F \quad \text{and} \quad \rho\nabla u=0 \tag{5}$$

where ρ is the fluid density, p – the fluid pressure, and μ – the dynamic viscosity.

Boundary conditions and continuity conditions

Based on mass conservation and pressure balance, the flow velocity and the fluid pressure in two adjacent regions are equal. The Darcy flow area has a steady water supply. The ambient atmospheric pressure is 0.1 MPa. On the adjacent boundary between aquifer and fault fracture zone, these conditions are given:

$$p_{\mathrm{D}}=p_{\mathrm{B}} \quad \text{and} \quad u_{\mathrm{D}}=u_{\mathrm{B}} \tag{6}$$

where p_{D} and p_{B} is the fluid pressure in Darcy linear flow and Brinkman non-linear flow, respectively, and u_{D} and u_{B} is the Darcy velocity in Darcy linear flow and Brinkman non-linear flow, respectively.

On the adjacent boundary between the fault fracture zone and the tunnel working face, these conditions are presented:

$$p_{\mathrm{B}}=p_{\mathrm{NS}} \quad \text{and} \quad u_{\mathrm{B}}=u_{\mathrm{NS}} \tag{7}$$

where p_{B} and p_{NS} is the fluid pressure in Brinkman non-linear flow and Navier-Stokes turbulence, respectively, and u_{B} and u_{NS} is the Darcy velocity in Brinkman non-linear flow and Navier-Stokes turbulence, respectively.

The subscript D represents the Darcy linear flow, B represents the Brinkman non-linear flow, and NS represents the Navier-Stokes turbulence. Combined with the formula and practical engineer, the COMSOL Multiphysics is employed to establish a numerical model by coupling the three stages of fluid-flow, and analyze the evolution process of fault water inrush in each stage.

Model establishment and numerical simulation

Model establishment

The total length of one tunnel is 10.528 km, and the maximum buried depth is 670 m. The whole tunnel is located in a single side downhill, which crosses 4.873 km carbonate rock stratum, accounting for 46.3% of the total length of the tunnel. There are 15 faults in the geological layer of the tunnel area, 11 of which are located in the carbonate formation. The construction area of the tunnel is the bottom layer of soluble rock. The maximum predicted water inflow is 746902 m^3 per day and the normal water inflow is 177298 m^3 per day.

Based on the engineering background in the F11 water-rich fault of the karst tunnel, the numerical model of 2-D fault water inrush is established. The model consists of three parts. The upper aquifer is 100 × 30 m, the width of the fault rupture zone is 4 m, the dip angle is 75°, the tunnel is excavated from the left boundary, and the height of the building boundary is 5 m. According to the hydro-geological conditions, the seepage boundary of the model is set. The boundary on both sides of the aquifer is fixed water pressure 4.1 MPa, the upper boundary has stable water pressure, and the other external boundary is non-flowing boundary. The initial water pressure of the aquifer and fault fracture zone was set at 4.1 MPa. The upper part of the stress field is fixed constraint boundary, the two sides are roller supported boundary, the tunnel excavation palm face and the air face are free boundary, and the atmospheric pressure is constant 0.1 MPa. The dynamic viscosity is 0.001, and the porosity in aquifer linear flow is 0.14, and the porosity in non-linear flow in fracture zone is 0.348. The numerical model is shown in the fig. 1, and A-B-C-D is the monitoring point of water pressure and velocity.

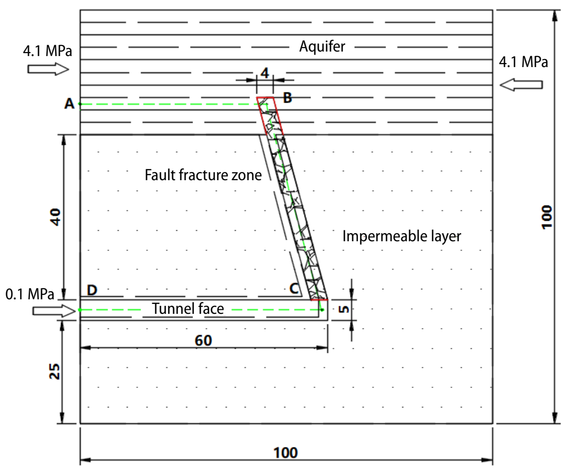

Figure 1. Numerical model of water inrush in karst fault tunnel

There are 1238 domain units and 197 edge units in the model. According to the boundary conditions and continuity conditions in the previous section, the numerical model is established, and the steady-state solver and the transient solver are used to calculate the water pressure and velocity of the three flow fields. Rock permeability is a dynamic process. Six working conditions are set in the study. The γ is the ratio of the permeability of fault fracture zone to the permeability of aquifer, and the values are 0.01, 0.1, 1, 10, 100,1000.

$$\gamma = \frac{k_\mathrm{B}}{k_\mathrm{D}} \tag{8}$$

where k_B is the permeability of fault fracture zone and k_D is the permeability of aquifer, with the value of 2.1×10^{-11}.

Numerical simulation and results analysis

The numerical simulation of water pressure is shown in fig. 2. When $\gamma \le 1$, the minimum water pressure in the model is $6.88\cdot10^4$ Pa; When $\gamma > 1$, the minimum water pressure in the model is $6.88\cdot10^4$ Pa, the minimum water pressure increases in accordance with the increase of

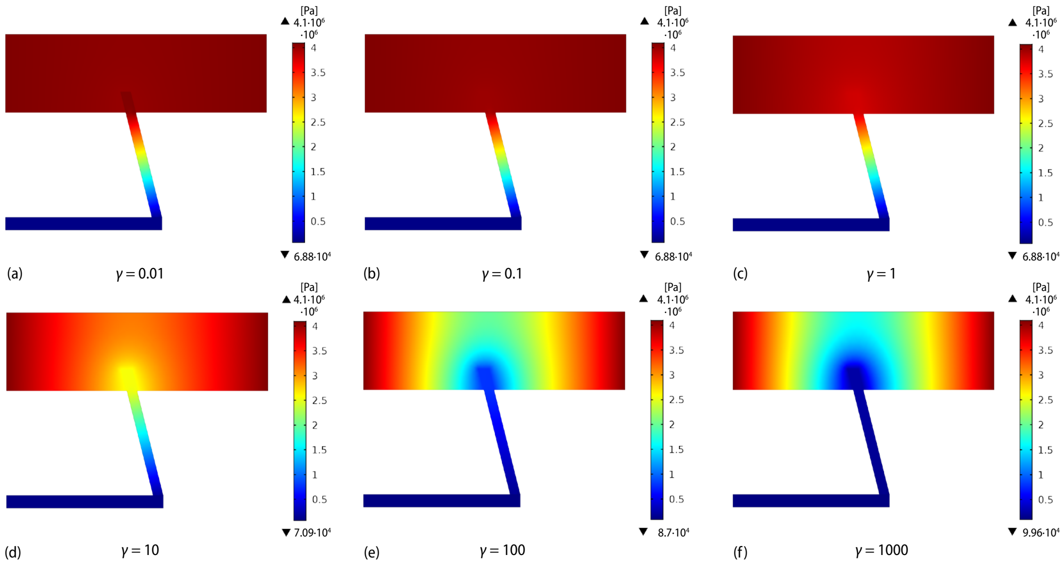

Figure 2. Numerical simulation of water pressure

γ, but they are all less than the atmospheric pressure 0.1 MPa of tunnel working surface. In addition, the water pressure at the adjacent boundary between the aquifer and the fault gradually decreases, and the continuous color of the cloud indicates that the adjacent flow field satisfies the condition of water pressure continuity. The water pressure in the working face of the tunnel is always less than 0.1 MPa, which is the atmospheric pressure connecting to the outside world.

The numerical simulation of flow rate is shown in fig. 3. With the increase of γ, the maximum value of the flow rate gradually increases, and it is concentrated in the adjacent area of the aquifer and the fault, at the same time, the flow rate in the working face of the karst tunnel also increases, and the fluid velocity under the sixth working condition reaches 0.75 m/s.

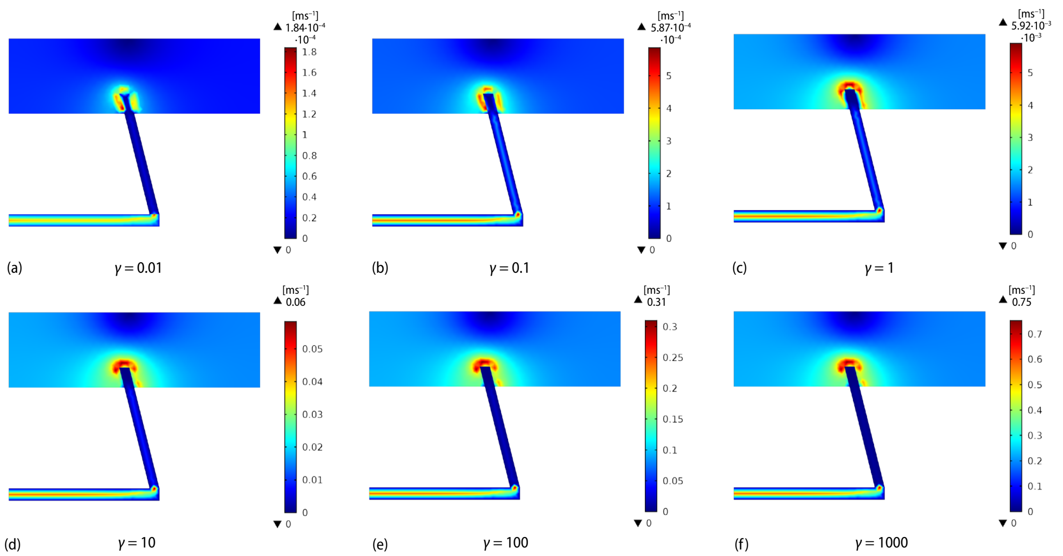

Figure 3. Numerical simulation of flow rate

In order to understand the change trend of water pressure and fluid velocity in aquifers and fracture zones more intuitively, the figs. 4 and 5 are obtained through the post-processing function of the results. It can be seen from the model diagram and the curve diagram that the fluid-flows from the aquifer to the fault, and the operating conditions with different permeability ratios are compared, indicating that the fluid-flows into the fault more easily. In the fault, the fluid-flows through the water guide channel and reaches the tunnel face, and the water pressure and flow rate gradually decrease.

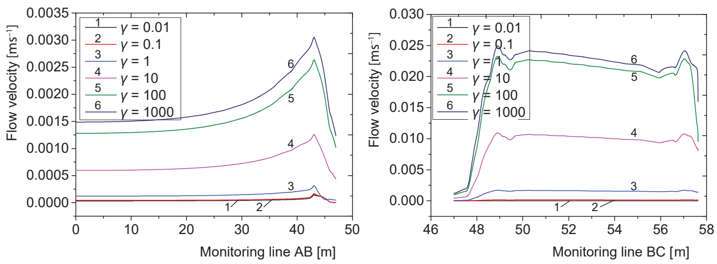

Figure 4. Flow velocity on monitoring line A-B-C

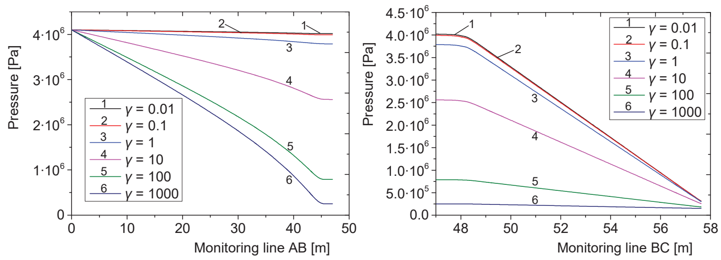

Figure 5. Water pressure on monitoring line A-B-C

Figure 6 shows the situation in the working face of the tunnel. The water pressure is constant at atmospheric pressure 0.1 MPa, and the maximum velocity is 4.2×10^{-5} m/s, which can be ignored, indicating that no water inrush occurs in the working face of the tunnel under this working condition.

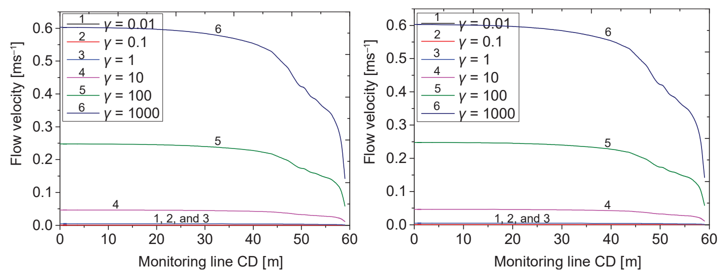

Figure 6. Numerical results in working face of the tunnel

Conclusions

In this work, combined with engineering practice, the COMSOL multiphysics coupling software was used to establish the non-linear seepage model to simulate lagging water inrush disasters in karst faults. The Darcy law is used to describe the steady flow of aquifer fluid, and the Brinkman equation is used to describe the slow flow of porous media in the fault, and the Navier-Stokes is used to describe the fast flow in the flow channel. By setting six fault permeability conditions, the water pressure and velocity of the three flow fields are analyzed and compared. It is shown that the water pressure and flow velocity change significantly with the change of fault permeability.

Acknowledgment

This study is sponsored by the National Natural Science Foundation of China (51904091, 52004082, 51904113), the Program for Science & Technology Innovation Talents in Universities of Henan Province (19HASTIT047), the Science and Technology Project of Henan Province (182102310012), the Fundamental Research Funds for the Universities of Henan Province (NSFRF200302), the Foundation for Higher Education Key Research Project by Henan Province (19A130001), the Scientific and Technological Development Project for Coal Mine Safety Production by Henan Province (HN19-59), the Postdoctoral Research Projects of Henan Province, the Natural Science Foundation of Henan Province (202300410170).

Nomenclature

k – permeability, [m^2]
p – fluid pressure, [MPa]
Q_m – source and sink term, [–]

Greek symbol

ρ – fluid density, [kgm^{-3}]

References

[1] Shen, W. L., *et al.*, Prediction of Relative Displacement for Entry Roof with Weak Plane Under the Effect of Mining Abutment Stress, *Tunnelling and Underground Space Technology*, *71* (2018), Jan., pp. 309-317
[2] Xue, Y., *et al*., Productivity Analysis of Fractured Wells in Reservoir of Hydrogen and Carbon Based on Dual-Porosity Medium Model, *International Journal of Hydrogen Energy*, *45* (2020), 39, pp. 20240-20249
[3] Zhang, Y., *et al.*, The Application of Short-Wall Block Backfill Mining to Preserve Surface Water Resources in Northwest China, *Journal of Cleaner Production*, *261* (2020), July, pp. 121232
[4] Yang, T. H., *et al.*, A Non-Linear Flow Model Based on Flow Translation and Its Application in the Mechanism Analysis of Water Inrush Through Collapse Pillar, *Journal of China Coal Society*, *42* (2017), 2, pp. 315-321
[5] Li, L. J., *et al.*, Mechanism of Water-Inrush Through Fault, *Journal of China Coal Society*, *2* (1996), 2, pp. 119-123
[6] Xue, Y., *et al.*, Investigation of the Influence of Gas Fracturing on Fracturing Characteristics of Coal Mass and Gas Extraction Efficiency based on a Multi-physical Field Model, *Journal of Petroleum Science and Engineering*, *206* (2021), Nov., 109018
[7] Li, L. C., *et al.*, Numerical Analysis of Pathway Formation of Groundwater Inrush from Faults in Coal Seam Floor, *Chinese Journal of Rock Mechanics and Engineering*, *28* (2009), 2, pp. 290-297
[8] Sun, J., *et al.*, Floor Fault Water-Inrush Prediction Based on Catastrophe Analysis of Micro-Seismic Signals, *Journal of China Coal Society*, *38* (2013), 8, pp. 1404-1410
[9] Liu, H. L., *et al.*, Investigation on Failure and Water Inrush from Roof of 5th Coal Seam in Fangezhuang Coal Mine, *Journal of Mining & Safety Engineering*, *26* (2009), 3, pp. 332-335
[10] Li, H. Y., *et al.*, The Seepage-Flowing Conversion Mechanism of the Fault Lagging Water Inrush and Its Numerical Simulation, *Journal of Mining & Safety Engineering*, *34* (2017), 2, pp. 323-329
[11] Guo, W. J., *et al.*, Study on Fault Water Inrush Mechanism and Nonlinear Seepage-Stress Coupling, *Journal of Shandong University of Science and Technology*, *36* (2017), 6, pp. 1-7
[12] Cao, Z. Z., *et al.*, Joint Bearing Mechanism of Coal Pillar and Backfilling Body in Roadway Backfilling Mining Technology, *Computers, Materials & Continua*, *54* (2018), 2, pp. 137-159
[13] Xue, Y., *et al.*, Analysis of Deformation, Permeability and Energy Evolution Characteristics of Coal Mass around Borehole after Excavation, *Natural Resources Research*, *29* (2020), 5, pp. 3159-3177
[14] Liu, J., *et al.*, Numerical Evaluation on Multiphase Flow and Heat Transfer during Thermal Stimulation Enhanced Shale Gas Recovery, *Applied Thermal Engineering*, *178* (2020), Sept., 115554

Paper submitted: March 29, 2020
Paper revised: June 25, 2020
Paper accepted: August 9, 2020